Seismic Assessment and Retrofitting of an Old Reinforced Concrete Frame Building

Ana Rodrigues
ana.beatriz.rodrigues@tecnico.ulisboa.pt
Instituto Superior Técnico, Universidade de Lisboa, Portugal, 2020

ABSTRACT: The consequences of an earthquake depend heavily on the vulnerability of buildings. As Portugal has been affected by major seismic events, some of which have caused serious damage, it is essential that the seismic performance of the structures should be assessed and inproved in order to mitigate the impact of an eventual earthquake. However, an adequate seismic design was not fully implemented in the design of new buildings until the 1980's, so reinforced concrete buildings constructed between 1950 and 1980, represent an identified seismic risk. Thus, the seismic assessment of these buildings is essential to determine the need of retrofitting. The objective of this dissertation is to evaluate the main deficiencies of a reinforced concrete frame building considered representative of the previous period, in order to propose a retrofitting strategy with the aim of verify the seismic performance requirements defined in Part 3 of Eurocode 8. The structure was modeled in SAP2000 software and evaluated by means of a nonlinear static analysis, according to the N2 method proposed in Part 1 of Eurocode 8. The presence of masonry infills has been ignored in the design and assessment of buildings, however, it has been broadly shown that presence of infill panels has a significant influence on global structural behavior when subjected to seismic action. In this dissertation, masonry infills were modeled using a non-linear relationship and their influence on the behavior of the building was studied.

Keywords: reinforced concrete building, masonry infills, seismic assessment, seismic retrofitting, nonlinear static analysis, N2 method

1 INTRODUCTION

Over the years, there are several episodes that prove the seismic activity to which Portugal mainland is subject. The relatively low probability of occurrence of major earthquakes in Portugal could explain the passivity with which the seismic risk has been faced. However, the catastrophic consequences of such event, mostly due the vulnerability of the existing buildings, impose the need to create measures to reduce the consequences of an earthquake.

The seismic vulnerability of buildings is mainly related to the time of construction and the standards in force at the time. In 1958, the first portuguese norm in which seismic resistance was considered in the design of buildings [1], the *Regulamento de Segurança das Construções contra Sismos*, was implemented. However it was based on simplified methods, inadequate in the light of today's knowledge. According to [2], buildings built in Portugal between 1950 and 1980 have a seismic performance below 50% of that required in current standards, thus showing the high seismic vulnerability of buildings built in this period. The importance of ductility in structural design was only introduced in 1983 by the REBAP (*Regulamento de Estruturas de Betão Armado e Pré-Esforçado*) [3]. Although currently the greatest threat from seismic activity to human life is in existing buildings, the focus of seismic engineering attention still remains mainly on new buildings, however, the retrofitting of the existing buildings has received increasing attention. In fact, nowadays, after years of experience accumulated in seismic engineering, the seismic resistance design adds very little to the construction cost of a new building. On the other hand, seismic retrofitting cost of old existing buildings is normally a large fraction of the building refurbishment cost. Seismic assessments of existing buildings in areas of moderate to high seismic activity is fundamental in order to determinate the need to retrofit or not. The adequate seismic assessment of an existing building implies the consideration of all elements of the building that influence its seismic performance, both structural and non-structural [4]. The presence of masonry infills in reinforced concrete buildings is very common, nevertheless, and even today, during the design process of new buildings and in the assessment of existing ones, infills are generally considered to be non-structural elements, and their

influence on the structural response is ignored. However, their influence is recognized in global behavior of RC frames subjected to seismic loadings (Asteris and Cotsovos 2012 [5]).

The main objective of this study was to model and analyze the seismic performance of a framed reinforced concrete (RC) building, representative of buildings designed and built between 1950 and 1960 in Portugal, not considering and considering the masonry infills, in order to study the damage distribution and a possible retrofitting solution. For this, a nonlinear static analysis was performed using the structural analysis software SAP2000 (CSI, 2019) with the aim to fulfil the seismic performance requirements defined in part 3 of Eurocode 8.

This work begins with a brief description of the building chosen as case-study. Then a summary of the main modeling strategies is presented. Afterwards, the seismic assessment of the building is performed, and the results discussed. A brief review of the proposed retrofitting strategy is presented and finally some final considerations are made.

2 OVERVIEW OF THE CASE STUDY

The building studied is an six-storey (ground floor plus five storeys above ground) reinforced concrete (RC) frame building located in Lisbon (Portugal) that was designed and built in the late 1950's (figure 1). Its plan dimensions are 17.80m in the X direction, and 10.70m in Y direction. Total building height is 20.60m.

Figure 1 – Case-study building (north elevation).

The structure was designed as a frame system, featuring a non-regular distribution of columns (figure 2).

This building has the following characteristics:

(i) Interior columns oriented in the Y direction;
(ii) Reduction of the column section in height;
(iii) Smooth reinforcement bars;
(iv) Masonry infills with a relatively regular distribution in height.

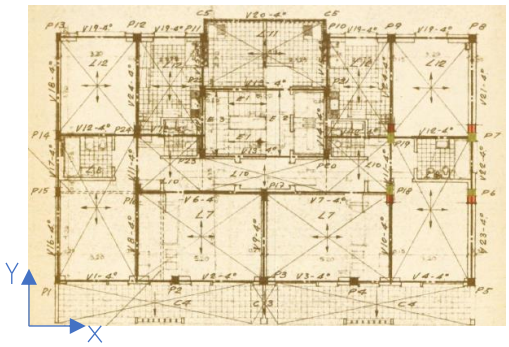

Figure 2 – Directions identification and identification of structural elements at the third floor.

Typically, most RC buildings built in the 1950's contain an array of non-ductile detailing of the reinforcing steel. Some inadequate reinforcement detailing conditions that were noticed in a preliminary assessment of the case-study building are:

(i) The number and spacing of the columns transverse reinforcement ties is generally insufficient, originating the premature failure of the section due to shear and bulcking of the bars under compression. Moreover, the distance between consecutive longitudinal bars restrained by ties exceeds the EC8-1 [6] limit (200mm);
(ii) The transverse reinforcement in the beams is manifestly insufficient and the use of bent longitudinal beam bars in joints (instead of stirrups) originates an undesirable behavior of the system in case of stress reversal, since the number of stirrups is not enough to guarantee the beam-column joints deformation with the necessary ductility [7];
(iii) The column bars are spliced and anchored inside the beam-column joint, which is a critical region for the behavior of the frame;
(iv) Reinforced concrete elements have smooth longitudinal reinforcing bars, which increase the bond-slip effect.

3 COMPUTATIONAL MODELLING OF THE BUILDING

The three-dimensional model of the case-study building was developed using SAP2000 (CSI, 2019), which allows different types of analysis. The ones used in this study were modal analysis (for the dynamic characterization of the structure), and nonlinear static ("pushover") analysis based on the procedure defined in Part 1 of Eurocode 8 (EC8-1) [6], the N2 method.

3.1 Materials

In nonlinear analysis methods, the nonlinear behavior of materials is reproduced by their constitutive relationships, which allows to simulate more

rigorously the nonlinear behavior of the structure. The properties of the adopted materials are presented below.

3.1.1 Concrete

Due to an inadequate detailing of the transverse reinforcement on the RC elements (columns and beams), it was assumed for the original model a stress-strain relationship of an unconfined concrete. According to the project's specification, the mean concrete compressive strength is 30 MPa, which is approximately equivalent to C20/25 strength class. The main properties of the unconfined C20/25 concrete are as follows in table 1.

Table 1 – Properties of C20/25 concrete considered.

Concrete	***C20/25 Unconfined***
Tangent Modulus of Elasticity (GPa)	30
Poisson's Ratio	0.20
Mean compressive strength (MPa)	28.0
Mean tensile strength (MPa)	2.2
Compressive strain at peak	0.0020
Ultimate strain	0.0035

In figure 3 it is possible to observe the difference between the unconfined concrete model, which was considered, and the confined model proposed by Mander et al. (1988) [8].

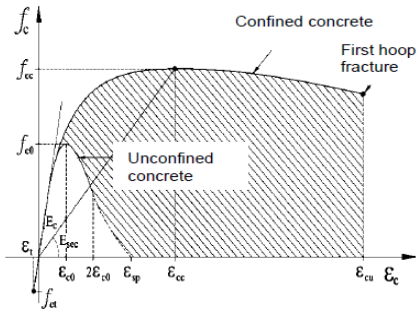

Figure 3 – Stress-Strain relationship for unconfined and confined concrete (adapted from Mander et al. (1988), [8]).

3.1.2 Steel

In the project's specification no reference was found about the steel class used. However, since the building was built in the late 1950's, and according to the regulation that was in force, the *Regulamento de Betão Armado* (RBA) [9], the reinforcement bars are smooth, with an ultimate strength of 370 MPa, and a yield strength corresponding to 60% of this, i.e. 222 MPa.

The main properties assumed were as defined in table 2.

Table 2 – Steel properties considered.

Steel	
Modulus of Elasticity (GPa)	210
Poisson's Ratio	0.30
Yield strength (MPa)	222
Minimum ultimate strength (MPa)	370
Hardening strain	0.0150
Minimum strain at breaking	0.2400

The model proposed by Park and Paulay (1975) [10] was adopted as the constitutive relationship for steel (figure 4).

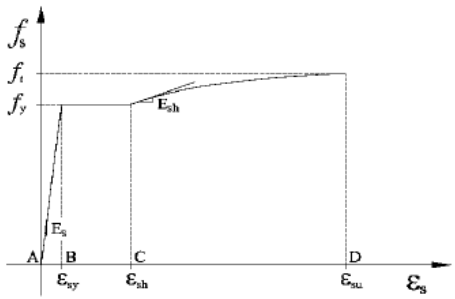

Figure 4 – Stress-strain relationship for steel (adapted from Park-Paulay (1975), [10]).

3.2 Modelling of structural and non-structural elements

The columns and beams of the case-study building were modelled as linear frame elements. The cross-sections were modelled with SAP2000 Section Designer (CSI, 2019). The slabs were modelled through the imposition, in each floor, of a rigid diaphragm behavior, since they are solid slabs, so these present a very reduced deformability in its plane. Regarding the foundations, in a conservative way, as suggested in [11], columns at the base were modelled with restrained translations and rotations about all directions.

The masonry infills were modeled using diagonal struts that simulate the compression to which these elements are subjected during the seismic action (figure 5).

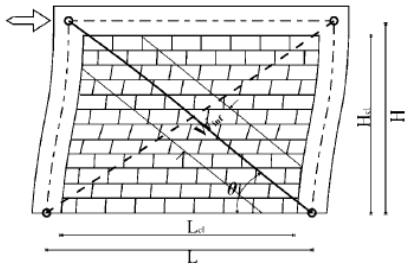

Figure 5 – Modelling of solid panel with strut along the compressed diagonal, (adapted from Fardis (2009), [12]).

According to [13], the strut has the same thickness as the masonry infill, t_w, and width in the plane of the infill, b_w, (or w_{inf}), is given by equation (1).

$$b_w = \frac{0{,}175 L_{cl}}{\cos(\theta)(\lambda H)^{0,4}} \quad (1)$$

Where:

$$\lambda = \left(\frac{E_w t_w \sin(2\theta)}{4 E_c I_c H_{cl}}\right)^{1/4} \quad (2)$$

Where L_{cl} is the clear horizontal dimension of the infill panel; θ is the inclination of the diagonal; H and H_{cl} is the theoretical and clear column height, respectively; E_c and E_w is the elastic modulus of the column concrete and of masonry infill, respectively; I_c is the moment of inertia of the column section about the normal to the infill panel and t_w is the infill thickness.

The openings in the masonry infills were considered through a reduction factor, λ_{op}, of infill width proposed by Al-Chaar [14], (equation (3)).

$$\lambda_{op} = 0{,}6\left(\frac{A_o}{A_p}\right)^2 - 1{,}6\left(\frac{A_o}{A_p}\right) + 1 \quad (3)$$

Where A_o is the opening area, and A_p the infill panel.

3.3 Nonlinear modelling strategy

Nonlinear behavior is modeled essentially through two groups of strategies: concentrated plasticity models, with inelastic behavior concentrated at elements extremities, or distributed plasticity models [15]. In the case-study building, the nonlinear behavior of the elements was modeled using rigid-plastic hinges at the respective ends (concentrated plasticity), since localized inelastic deformations in beams and columns at their ends holds acceptably close to their real behavior [16]. It should be noted that the concentrated plasticity model was adopted not only for structural elements, but also for non-structural elements.

3.3.1 Modelling of nonlinear behavior of columns and beams

The nonlinear behavior of columns and beams was performed using plastic hinges at the ends of the elements, where moment-curvature relationships were defined. Plastic hinges were implemented automatically using the idealized bilinear moment-curvature relationship of the "CALTRANS Flexural Hinges". For beams, only the bending moment M3 was considered, and for columns was considered plastic hinges with an interaction P-M2-M3.

As for the definition of plastic hinge length, the equation (4) proposed by Paulay and Priestley [17] was adopted, with a reduction of 50% due to the use of smooth steel rebars [18].

$$L_p = 0.04L + 0.011 f_{sy} d_{bl} \quad (4)$$

Where L is the length of the reinforced concrete element, f_{sy} is the yielding strength of the reinforcement (in MPa) and d_{bl} is the diameter of the main longitudinal reinforcing bars.

3.3.2 Modelling of nonlinear behavior of masonry infills

The nonlinear behavior of the masonry infills was performed by means of concentrated plastic hinges at diagonal struts extremities, where the axial force-displacement relationship proposed by Panagiotakos and Fardis [19] (figure 6) was defined.

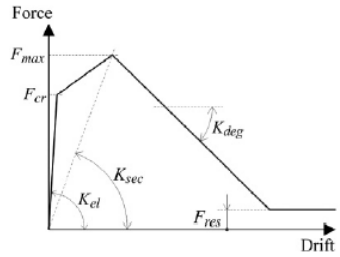

Figure 6 – Quadrilinear force-displacement relationship of the diagonal struts (in compression), (adapted from Celarec et al, 2012 [20]).

4 SEISMIC ASSESSMENT OF THE EXISTING RC STRUCTURE

Based on the computational modeling of the case-study building, in this section the results obtained by the modal dynamic analysis and nonlinear static ("pushover") analysis are described.

4.1 Modal dynamic analysis

The analysis to obtain the frequencies and vibration modes was performed using SAP2000 (CSI, 2019). In this analysis, two distinct computational models were studied: considering the presence of masonry infills or neglecting their influence. Table 3 presents the frequency values for the first three vibration modes in the model without and with masonry infills, as well as the experimental results developed in [21].

Table 3 – Frequencies and vibration modes.

	Frequency [Hz]		
Mode	Without infills	With infills	Experimental results
1	1.29 (X)	3.18 (Y)	4.00 (Y)
2	1.38 (X)	3.20 (X)	4.40 (X)
3	1.82 (R)	4.69 (R)	5.12 (R)

Table 3 shows the frequencies associated to the model with infills are closest to the experimental results.

The masonry infills model frequencies are higher than the ones corresponding to the model without infills, which is in line with expectations, since the consideration of masonry infills makes the structure more rigid and leads to higher vibration frequencies.

4.2 Nonlinear static ("pushover") analysis

Nonlinear static analyzes are essentially an extension of the lateral force analysis method for the nonlinear regime. This analysis is carried out under constant gravitational loads and monotonically increasing lateral loading applied on the masses of the structural model. According to EC8-1 [6], at least two vertical distributions of lateral loads must be applied: a "uniform" distribution, which consists of lateral forces proportional to the mass regardless of height; and a "modal" distribution, proportional to the lateral forces corresponding to the prevailing translation vibration mode in the direction in which the analysis is carried out. In order to assess the capacity of the structure, pushover analyzes were performed based on the N2 method proposed by Fajfar [22] and indicated in Part 3 of Eurocode 8 (EC8-3) [23]. The seismic assessment was performed by comparing the capacity with the demand at the significant damage (SD) limit state, as indicated by the Portuguese National Annex of EC8-3[23], with a reduced return period of 308 years for the seismic action.

4.2.1 Capacity curves

From pushover analysis, the structure's capacity curves were obtained for the two types of models: with and without masonry infills. In the presented analyzes (figure 7) it was not possible to reproduce the effect of loss of resistance after reaching the maximum basal shear force so the analysis was considered only until the first plastic hinge of a column reach the LS-Life Safety level, (associated to the significant damage (SD) limit state). It should be noted that the analysis was carried out in the negative and positive direction of both directions, but since the results are similar, only those obtained in the negative direction are presented. It is important to note that, due to the reasonable symmetry, although not total, the analyzes in the X + and X- directions are similar as in the Y + and Y- directions.

Figure 7 shows that in both directions the model with masonry infills leads to values of base shear well above the values of the model without masonry infills, so the consideration of masonry walls substantially increases the resistance and stiffness of the structure. Regarding the model with masonry infills, it appears that uniform loading leads to higher basal force values, which makes modal loading the most conditioning load for the case-study building.

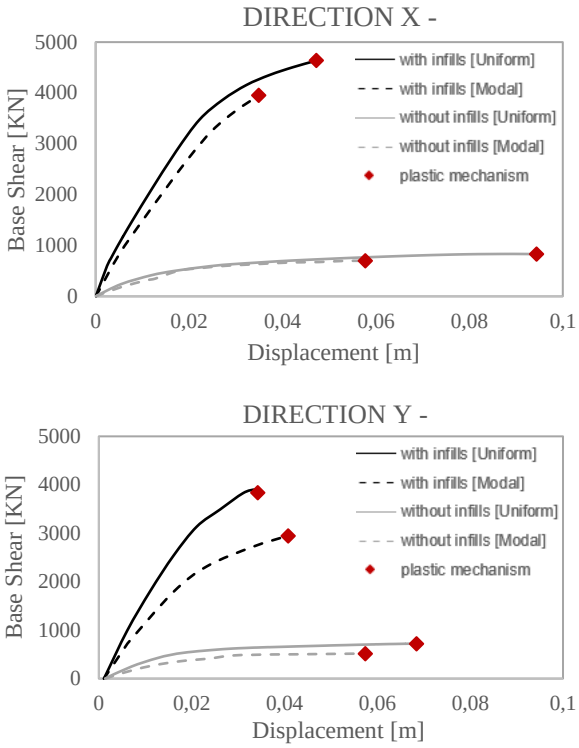

Figure 7 – Capacity curves in X- and Y- directions.

4.2.2 Damage distribution

In addition to obtaining the capacity curves, the pushover analysis allows to monitor the damage distribution of the structure. To illustrate this, in figure 8, the damage distributions for uniform loading in the X- direction of the models with and without masonry infills are compared for the ultimate displacement correspondent to the SD limit state.

In the model with masonry infills, one can notice that several plastic hinges of the base columns reach the LS-Life Safety level. In the model without masonry infills, the plastic hinges of the fourth floor columns, (the floor where the reduction of their section occurs), are the ones that reach the LS-Life Safety level. In this model there are several beams with enter in the nonlinear behaviour with the formation of the plastic hinges, with the levels of inelastic behaviour being higher than those observed in the model with masonry infills. This imbalance between the strength of the columns in relation to the beams in the beam-column joints of the model with masonry infills, gives the gantry little capacity to redistribute efforts, generating local mechanisms that can lead to the premature brittle collapse, global or local, of the structure without the desired exploration of their nonlinear behavior.

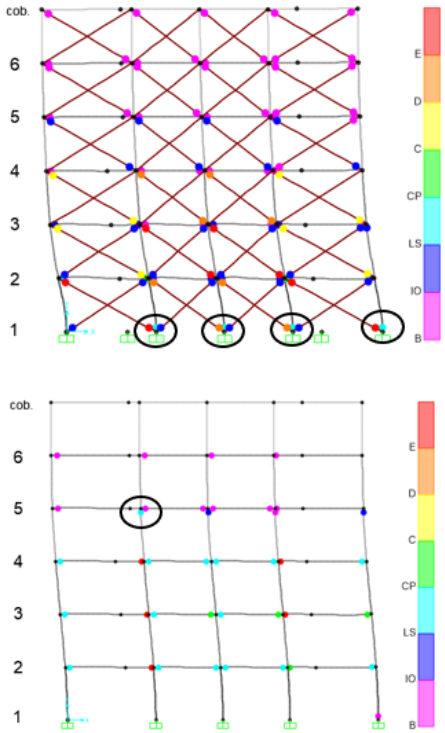

Figure 8 – Comparison of damage distribution between the model with and without masonry infills for uniform loading in the X- direction, (south elevation).

4.2.3 Ductile components

According to EC8-3 [23], the seismic assessment of ductile components/mechanisms of the structural elements is performed in terms of chord rotation capacity. The ultimate chord rotation capacity, θ_{um}, can be calculated, according to [23], from the following equation:

$$\theta_{um} = \frac{1}{\gamma_{el}} \left[\begin{array}{c} 0.016(0{,}3^{\upsilon}) \left[\frac{max(0.01;\omega')}{\max(0.01;\omega)} f_c \right]^{0{,}225} \cdot \\ \left(\min\left(9; \frac{L_v}{h}\right) \right)^{0{,}35} 25^{\left(\alpha \rho_{sx} \frac{f_{yw}}{f_c}\right)} (1.25^{100\rho_d}) \end{array} \right] \quad (5)$$

Where γel is equal to 1.5, υ is the normalized axial force, ω and ω' are the mechanical reinforcement ratio of the tension and compression longitudinal reinforcement, respectively, h is the depth of cross section, L_v is the shear span or ratio moment/shear at the end section, f_c and f_{yw} are the concrete compressive strength and the stirrup yield strength, respectively, ρ_{sx} is the ratio of transverse steel parallel to the direction x of loading, ρ_d is the steel ratio of diagonal reinforcement and α is the confinement effectiveness factor.

The chord rotation capacity corresponding to SD limit state (θ_{SD}) is 3/4 of the ultimate chord rotation θ_{um}, as indicated by EC8-3 [23].

4.2.4 Brittle components

The shear resistance was evaluated, as prescribed by EC8-3 [23], by means of cyclic shear resistance V_R, (equation (6)).

$$V_R = \frac{1}{\gamma_{el}} \left[\begin{array}{c} \frac{h-x}{2L_v} \min(N; 0{,}55 A_c f_c) + 1 - 0{,}05 \min\left(5; \mu_{\Delta}^{pl}\right) \cdot \\ \left[\begin{array}{c} 0{,}16 \max(0{,}5; 100\rho_{tot}) \cdot \\ \left(1 - 0.16 \min\left(5; \frac{L_v}{h}\right)\right) \sqrt{f_c} A_c + V_w \end{array} \right] \end{array} \right] \quad (6)$$

Where, γel is equal to 1.15, h is the depth of cross section, x is the height of compressed zone, L_v is the shear span or ratio moment/shear at the end section, N is the axial compression load, A_c is the element section area, f_c is concrete compressive strength, μ_{Δ}^{pl} is the rotation ductility factor, ρ_{tot} is the total ratio of longitudinal reinforcement and V_w is the contribution of transverse reinforcement to shear resistance.

4.2.5 N2 method

The N2 method combines the pushover analysis of a multiple degrees of freedom system with the inelastic response spectrum of an equivalent system with a single degree of freedom. This method assesses the structure in terms of available and necessary ductility using a seismic performance point as the verification criterion, i.e., a displacement in the building's control node (center of mass of the structure's top floor), which is denominated as target displacement, d_t.

Table 4 shows that only in models without infills the ultimate displacement, du, (displacement for which the first plastic hinge of a column reaches the LS-Life Safety level), is lower than the target displacement, d_t. One can observe, the increase of resistance and stiffness with the consideration of infills leads to the reduction of the target displacement. In all models with infills, the ultimate displacement (du) is higher than the target displacement (d_t), concluding that in terms of flexural behavior the structure's capacity of ductile components is greater than the demand.

Table 4 – Ultimate displacement and target displacement.

		With infills			Without infills		
		du [m]	d_t [m]		du [m]	d_t [m]	
X+	Uniform	0.041	0.018	✓	0.052	0.070	✗
	Modal	0.030	0.020	✓	0.043	0.075	✗
X-	Uniform	0.047	0.019	✓	0.094	0.077	✓
	Modal	0.035	0.021	✓	0.058	0.073	✗
Y+	Uniform	0.047	0.019	✓	0.026	0.057	✗
	Modal	0.048	0.027	✓	0.068	0.079	✗
Y-	Uniform	0.034	0.018	✓	0.068	0.075	✗
	Modal	0.041	0.028	✓	0.057	0.085	✗

4.2.6 Assessment of brittle mechanisms

The structure components must be verified for potential brittle mechanism that could lead to a premature collapse of the structure. In figure 9, for each capacity curve, the point at which the shear resistance is reached, as well as the target displacements are shown. Only the results in the X- and Y- directions are shown since in the remaining directions the shear resistance is higher than the demand, (only in models with masonry infills).

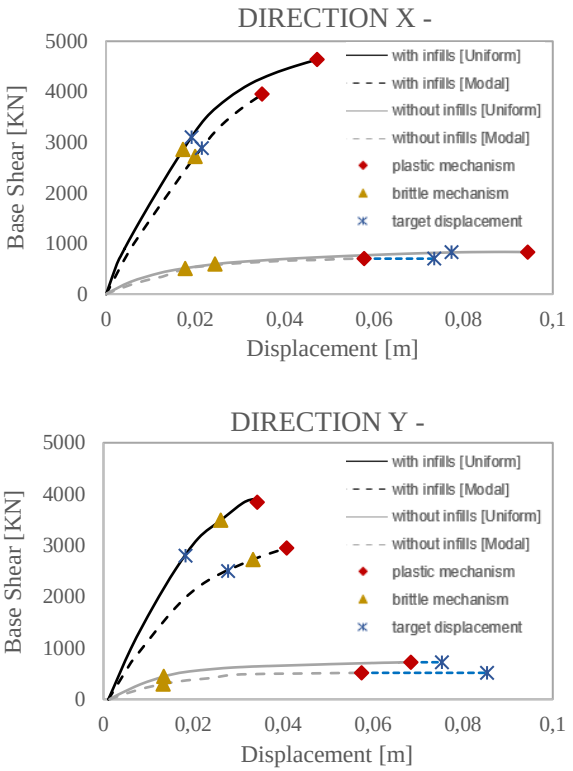

Figure 9 – Capacity curves in X- and Y- directions with the brittle mechanism and target displacement.

In without infills models, it is possible to observe that the top displacements associated to the brittle mechanism are, in general, considerably lower than those associated to the plastic mechanism, in contrast to what happens in models with infills, due to the greater stiffness of the structure. In this models, as in general for bending (plastic mechanism), brittle mechanism also occurs for top displacements lower than the target displacements, so the demand is greater than the capacity for both bending and shear strength. In with infills models, only in direction X-, both for uniform and modal loading, the target displacement is greater than the displacement associated to the brittle mechanism (demand greater than the capacity).

As the with infills model, the one that most closely matches the real behavior of the case-study building, the assessment of brittle mechanisms will only focus on this model, more specifically, on the with infills model with a modal loading in direction X-, as compared to uniform loading, this presents a slightly greater difference between the displacement associated to the brittle mechanism and the target displacement.

Columns conditioned by a brittle mechanism essentially belong to frame A and frame C (figure 10).

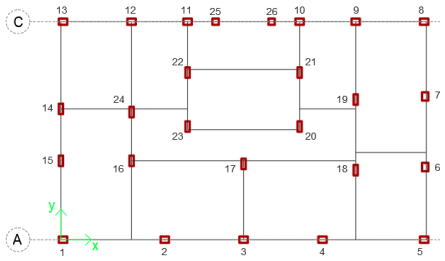

Figure 10 – Frame identification (first floor plan).

Figure 11 identifies the frame A and frame C columns with a shear strength for target displacement, V_2^{dt}, greater than the cyclic shear resistance, V_R, (i.e. columns with V_2^{dt}/V_R >100%).

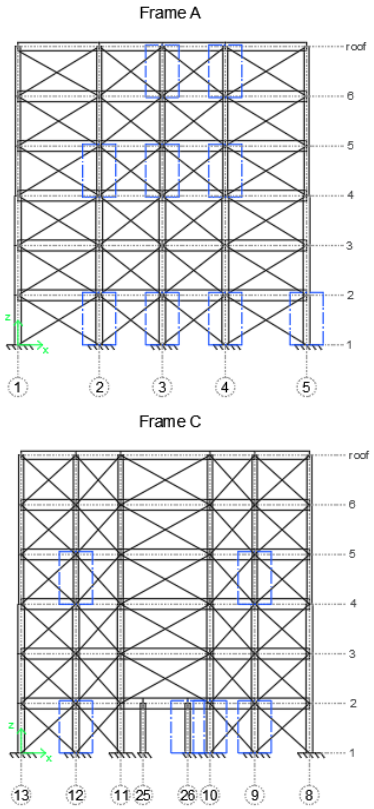

Figure 11 – Columns with V_2^{dt}/V_R >100% from frame A and frame B.

From figure 11, one can observe that the brittle mechanism occurs mainly in the base columns, where

the moment/shear ratio in the end section (L_v) is greater, in the fourth floor, where there is a strong reduction of the column section stiffness caused by the discontinuity in heigh of the section and by the reduction of the longitudinal reinforcement, and in the last floor, where the reduction of the section is accompanied once again by the decrease of the longitudinal reinforcement, and the beneficial effect from axial load is reduced.

5 SEISMIC RETROFITTING

The pushover analysis allowed to determine that, for the with infills model, in terms of ductile mechanisms the structure verifies the safety (capacity greater than the demand) for the severe damage limit state of EC8-3 [23]. The problem arises in terms of shear resistance in direction X- where it is verified that some of the vertical structural elements present a brittle behavior, failing to verify the safety (demand greater than the capacity) to the limit state of severe damages. Based on this conclusion, the reinforcement strategy will involve adopting a reinforcement solution by jacketing with CFRP.

Jackets of externally bonded CFRP is a quick and easy solution, which translates into a significant decrease of indirect costs, namely the costs associated to the interruption of occupation, and allows the increase of the shear resistance. Although the material used in this reinforcement solution has a high cost, at the intervention level, it is compensated mainly by the decrease in costs related to the vacancy of the structure to be reinforced.

5.1 Shear strength after structural reinforcement with CFRP

According to EC8-3 [23], the total shear capacity, controlled by the stirrups and the CFRP, is evaluated as the sum of a contribution from the existing concrete member (V_R), with another contribution due to CFRP ($V_{Rd,f}$). The total shear capacity may not be taken greater than the maximum shear resistance of the concrete member, $V_{R,max}$. For rectangular section elements, fully wrapped, the CFRP contribution ($V_{Rd,f}$) to the total shear capacity, is calculated by equation (7).

$$V_{Rd,f} = 0{,}9d.f_{fdd,e}.2.t_f.\left(\frac{w_f}{s_f}\right)^2.(\cot\theta + \cot\beta).\sin\beta \quad (7)$$

Where d is the effective depth, t_f is the thickness of the CFRP sheet, w_f is the width of the CFRP sheet, s_f is the spacing of CFRP strips (= w_f for sheets), θ is the strut inclination angle, β is the angle between the (strong) fiber direction in the CFRP sheet and the axis of the member, and $f_{fdd,e}$ is the design CFRP effective debonding strength.

Table 5 shows the mechanical properties of the CFRP jacketing reinforcement solution adopted.

Table 5 – Mechanical properties of the CFRP sheets used for the reinforcement (manufacturer S&P).

t_f [mm]	Nº of sheets	f_u [MPa]	E_f [GPa]	$\varepsilon_{u,f}$ [%]	$\varepsilon_{u,j}$ [%]
0.117	1	3800	240	1.55	0.93

In addition to the increase in shear strength, the jacketing of columns with CFRP, also increases the resistance of the element to compression through its confinement. The strength of confined concrete is evaluated from equation (8).

$$f_{cc} = f_c\left[1 + 3.7\left(\frac{f_l}{f_c}\right)^{0.86}\right] \quad (8)$$

Where, f_c is the concrete strength and f_l is the confinement pressure level.

The strain to which the new compressive strength of the confined concrete, f_{cc}, is verified is calculated using the equation (9).

$$\varepsilon_{cc} = \varepsilon_{c2}\left[1 + 5\left(\frac{fcc}{fc} - 1\right)\right] \quad (9)$$

And the ultimate strain of the extreme fiber of the compression zone is taken as:

$$\varepsilon_{cu,c} = 0.004 + 0.5\frac{f_l}{f_{cc}} \quad (10)$$

5.2 Application of structural reinforcement in the 3D model

After calculating the strength of confined concrete, f_{cc}, as well as the corresponding strain, ε_{cc}, and the ultimate strain of the extreme fiber, $\varepsilon_{cu,c}$, a new material was created in SAP2000 software (CSI, 2019) with the previous properties, which was replaced in all vertical structural elements in which a brittle mechanism occurs. This substitution led to columns that previously checked the condition $V_2^{dt} < V_R$ now failing to check it, needing to be reinforced as well. In figure 12, all columns belonging to frame A and frame C that need to be reinforced are identified.

As previously mentioned, the reinforcement solution used in the columns identified in figure 12 consisted of wrapping them with CFRP, more specifically, by applying a sheet of CFRP with a thickness of 0.117mm. Table 6 presents a summary of the reinforcement solution calculation, according to EC8-3 [23]. This summary is performed only for the columns that need reinforcement of axis 3 (V_2^{dt}/V_R >100%), these being representative of the other axes's columns that are also reinforced.

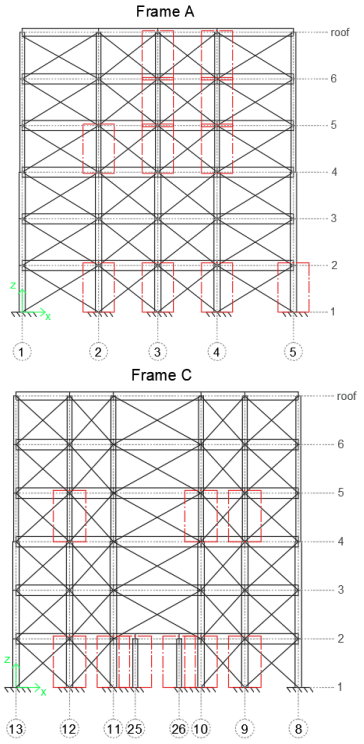

Figure 12 – Columns with V_2^{dt}/V_R >100% from frame A and frame B after changing the concrete properties.

Table 6 – Verification of criterion $V_2^{dt} \leq V_{Rd}$ after reinforcement with CFRP on the columns of axis 3.

Axis 3	$V_{R,max}$ *[KN]*	V_R *[KN]*	*CFRP* $V_{Rd,f}$ *[KN]*	V_{Rd} *[KN]*	V_2^{dt} *[KN]*	$V_2^{dt} \leq V_{Rd}$
1st floor	512.0	60.6	134.4	195.0	72.4	Checks
4th floor	298.7	25.1	95.9	120.9	30.1	Checks
5th floor	277.4	22.2	95.9	118.0	22.5	Checks
6th floor	251.1	8.6	95.9	104.5	12.2	Checks

From table 6, one can observe that in all columns of axis 3 that have been reinforced, the total shear capacity, V_{Rd}, is significantly higher than the shear strength acting when the target displacement is reached, V_2^{dt}. In fact, even considering the smallest available CFRP sheet thickness (0.117 mm), and the application of only 1 layer, the increase in shear strength due to the reinforcement is substantial, resulting in an increase in strength far beyond what is necessary. Thus, the amount of reinforcement required is reduced, and considerably less than that calculated with the minimum reinforcement of CFRP. Considering that, other solutions with a lower overall cost and whose increase in shear strength is also less must be explored.

6 FINAL CONSIDERATIONS

A six-storey RC building, located in Lisbon and built in the 1950's, was studied in this research. With a preliminary assessment of the structure some inadequate reinforcement detailing conditions and irregularity in elevation were noticed.

The nonlinear static analyzes performed on the building models enabled the identification of the main deficiencies of the structure that condition its seismic performance. Regarding the ductile mechanisms, it was found that in with infills models the capacity is greater than the demand, contrary to what happens in without infills models. From the analysis of brittle mechanisms, it was concluded that both with infills model, as without infills model, the rupture by shear strength in columns occurs without the full development of its deformation capacity, which is explained by the inadequate transverse reinforcement detailing. In all directions of the without infills models it was found that the brittle mechanisms occur for a displacement less than the target displacement, (demand greater than the capacity). In with infills models, it was observed that only in direction X- the demand is greater than the capacity, in terms of brittle mechanisms.

Focusing on the model in which the masonry infills are considered, since this is the closest to the real behavior of the structure when subjected to seismic action, and more specifically, the model with infills in direction X-, (capacity exceeds the demand in terms of the brittle mechanisms), a reinforcement solution was proposed. The columns reinforcement, in terms of shear strength, was carried out essentially on the columns at the base of the building, on the columns at the 4th floor (floor where the reduction of the column section occurs) and on the 6th floor columns (building's last floor). For this purpose, it was used the jacketing of these elements with CFRP sheets, as they were reinforced to increase shear resistance, and there was no need to increase the bending resistance. Although only one reinforcement layer and the thinner sheet were used, it was concluded that the resistance to shear strength after reinforcing the element considerably exceeds the shear strength acting when the target displacement is reached, V_2^{dt}, so it would be interesting to evaluate another reinforcement solution at a cost overall lower and an increase in shear resistance less than that verified using the minimum reinforcement by jacketing with CFRP.

It should be noted that the identification of the building elements to be reinforced demonstrates the advantage of nonlinear analyzes in the scope of the seismic assessment and retrofit of existing structures. In the case-study building, they allowed to clearly identify the structure's deficiencies in a very localized way, allowing with a localized intervention, so implying lower costs, to significantly improve the structure's seismic performance.

Finally, it should be noted that knowledge of all building elements, structural and non-structural, is

essential to assist practitioners in the assessment and retrofit of existing buildings, with the aim of reducing their vulnerability to seismic action and mitigating the consequences of a possible earthquake.

7 REFERENCES

[1] Ministério das Obras Públicas (1958) Regulamento de Segurança das Construções contra os sismos. Decreto-Lei 41658 Lisbon, Portugal [In Portuguese]

[2] J. Saraiva & J. Appleton (2006) Avaliação da Capacidade Sísmica de Edifícios de Betão Armado de Acordo com o Eurocódigo 8 – Parte 3. JPEE 2006, 4as Jornadas Portuguesas de Engenharia de Estruturas. [In Portuguese]

[3] Ministério da Habitação, Obras Públicas e Transportes (1983) Regulamento de Estruturas de Betão Armado e Pré-Esforçado. Decreto-Lei nº 349-C/83 Lisbon, Portugal [In Portuguese]

[4] A. Furtado, H. Rodrigues, A. Arêde (2015) Modelling of masonry infill walls participation in the seismic behavior of RC buildings using Opensees. International Journal of Advanced Structural Engineering. 7, 117–127 (2015). https://doi.org/10.1007/s40091-015-0086-5

[5] P. Asteris, D. Cotsovos (2012) Numerical investigation of the effect of infill walls on the structural response of RC frames. The Open Construction and Building Technology Journal, 6:164-181, DOI: 10.2174/1874836801206010164

[6] NP EN 1998-1 (2010) Eurocódigo 8: Projecto de estruturas para resistência aos sismos - Parte 1: Regras gerais, acções sísmicas e regras para edifícios. [In Portuguese]

[7] J. Appleton (2013) Estruturas de betão – volumes 1 e 2. Edições Orion, Portugal

[8] J. B. Mander et al. (1988) Theoretical Stress-Strain Model for confined concrete. ASCE Journal of Structural Engineering 114(8): 1804-1826.

[9] Ministério das Obras Públicas e Comunicações (1935) Regulamento do Betão Armado. Decreto-Lei nº 25948 de 16710/1935 [In Portuguese].

[10] R. Park & T. Paulay (1975) Reinforced Concrete Structures. J. Wiley, New York, USA. ISBN:9780471659174. https://pt.scribd.com/doc/39656154/Reinforced-Concrete-Structures-R-Park-T-paulay

[11] ASCE 7-05 (2006) Minimum design loads for buildings and other structures (7-05) including Supplement No.2. American Society of Civil Engineers, Reston, VA, USA. https://www.waterboards.ca.gov/waterrights/water_issues/programs/bay_delta/california_waterfix/exhibits/docs/dd_jardins/DDJ-148%20ASCE%207-10.pdf

[12] M. N. Fardis (2009) Seismic Design, Assessment and Retrofitting of Concrete Buildings: based on EN-Eurocode 8. Springer, Dordrecht

[13] R. J. Mainstone (1971) On the stiffness and strengths of infilled frames. Proceedings of the Institute of Civil Engineering, Supplement IV; 1971. P. 57-90.

[14] G. Al-Chaar, G. E. Lamb, M. A. Issa (2003) Effects of openings on structural performance of unreinforced masonry infilled frames.

[15] G. G. Deierlein, A. M. Reinhorn, M. R. Willford (2010) *Nonlinear Structural Analysis for Seismic Design – A Guide for Practicing Engineers.*

[16] K. Beyer, S. Simonini, R. Constantin, A. Rutenberg (2014) Seismic shear distribution among interconnected cantilever walls of different lengths. NEHRP Seismic Design Technical Brief No. 4. https://curee.org/projects/nehrp-jv/publications/nistgcr10-917-5.pdf

[17] T. Paulay, M. J. N. Priestley (1992) Seismic Design of Reinforced Concrete and Masonry Building. ISBN: 978-0-471-54915-4. In John Wiley & Sons Inc.: New York.

[18] C. Fernandes, J. Melo, H. Varum, A. Costa (2010). Comportamento cíclico de nós viga-pilar com armadura lisa. Aveiro, Portugal [In Portuguese] http://hdl.handle.net/10773/7162

[19] T. B. Panagiotakos, M. N. Fardis, (2001) Deformations of Reinforced Concrete Members at Yielding and Ultimate. ACI Structural Journal. https://doi.org/10.14359/10181

[20] D. Celarec, P. Ricci, M. Dolsek (2012) The sensitivity of seismic response parameters of the uncertain modelling variables of masonry-infilled reinforced concrete frames. Engineering *Structures*. https://doi.org/10.1016/j.engstruct.2011.11.007

[21] C. Palmeri (2019) Seismic performance assessment of old RC buildings in Lisbon.

[22] P. Fajfar & M. Fischinger "N2 – a method for nonlinear seismic analysis of regular buildings" Proceedings of the 9th World Conference in Earthquake Engineering, 1988, Vol.5, 111-116, Tokyo-Kyoto, Japan

[23] NP EN 1998-3 (2017) Eurocódigo 8: Projecto de estruturas para resistência aos sismos - Parte 3: Avaliação e reabilitação de edifícios. [In Portuguese]